The Korean Journal of Ceramics, 4 [2] 151 - 155 (1998)

Partial Conductivities, Nonstoichiometry and Defect Structure of a New Cathode Candidate $Y_{1-x}Ca_xFeO_{3-\delta}$

Chan-Soo Kim and Han-Ill Yoo

Solid State Ionics Research Laboratory, School of Materials Science and Engineering, Seoul National University, Seoul 151-742, Korea

(Received October 2, 1997)

The total electrical conductivity, ionic conductivity, and nonstoichiometry of a new cathode material $Y_{1-x}Ca_xFeO_{3-\delta}$ ($x=0.1$) were measured as functions of temperature ($900 \leq T/^{\circ}C \leq 1100$) and oxygen partial pressure ($10^{-16} \leq Po_2/atm \leq 0.21$). Isothermal variations of these properties with Po_2 support that the majority type of ionic defects are anti-Frenkel disorder which, however, has seldom been considered for perovskite-based oxides. The results are discussed in comparison with those reported on similar oxides.

Key words : $Y_{1-x}Ca_xFeO_{3-\delta}$, Electrical conductivities, Nonstoichiometry, Defect structure

I. Introduction

Perovskite-based oxides have been utilized in a variety of electrochemical devices, e.g., solid oxide fuel cells (SOFC).[1] Those oxides may generally be represented as $(A_{1-x}B_x)MO_{3-\delta}$ where "A" is normally rare earth elements (e.g., La, Y), "B" alkaline-earth elements (e.g., Ca, Sr) and "M" transition metals (e.g., Fe, Mn, Cr). Their basic electrochemical nature is mostly determined by B- and M-ions.[2] It is mainly because the transition metal ions have mixed valences. For instance, their electrical conductivity can be remarkably enhanced by substituting a lower-valence alkaline-earth metal ions (B) on A site.

We have been examining the electrochemical properties of Ca-doped $YFeO_{3-\delta}$ or $(Y_{1-x}Ca_x)FeO_{3-\delta}$ as a new cathode material for SOFC applications. It has been found that the oxide exhibits a maximum conductivity at $x=0.1$, apparently the solubility limit of Ca.[3] Furthermore, it is known that its thermal expansion coefficient (TEC), which is another important property for the SOFC application, can be controlled by varying Ca-content: TEC of the oxide can be adjusted to $11.0 \times 10^{-6}/^{\circ}K$ by doping Ca up to $x=0.1$,[4] which is quite compatible with that of 8 m/o-Y_2O_3-stabilized ZrO_2 (YSZ), $10.6 \times 10^{-6}/^{\circ}K$.[1] Additional advantage of $YFeO_3$ as the cathode may be that the formation of hazardous intercompounds with YSZ may be avoided due to their compositional commonality contrary to the currently used cathode $La_{1-x}Sr_xMnO_{3-\delta}$. The latter forms intercompounds such as $La_2Zr_2O_7$ to increase the cathodic overpotential.[1]

The purpose of the present work is to measure oxygen nonstoichiometry, δ, of $(Y_{0.9}Ca_{0.1})FeO_{3-\delta}$ as a function of oxygen partial pressure (Po_2) and temperature (T) in addition to its partial electrical conductivities. By combining all these properties, we wish to establish its equilibrium defect structure.

II. Experimental Procedure

Samples of $(Y_{0.9}Ca_{0.1})FeO_{3-\delta}$ were prepared via a conventional ceramic processing route. The starting powders of Y_2O_3 (Rare Metallic, Japan), Fe_2O_3 (Aldrich, USA) and $CaCO_3$ (Shimakyu Pure Chemical, Japan), all 99.99% pure, were thoroughly mixed in an appropriate ratio and calcinated at 900°C for 10 hrs in air and then sintered at 1350°C for 15 hrs in air. The apparent density of the sintered samples was 95% of the theoretical value.

The total electrical conductivity was measured by a conventional d.c. 4 probe method on a parallelepiped specimen which was cut out of the sintered sample, as detailed elsewhere.[3] The ionic partial conductivity was determined from an electron blocking electrochemical cell,[7]

$$Po_2', Pt \mid YSZ \mid Y_{0.9}Ca_{0.1}FeO_3 \mid YSZ \mid Pt, Po_2'' \quad (1)$$

by impedance spectroscopy combined with d.c. relaxation results. In this novel techique, a full spectrum over the frequency range of practically 0 to ∞ is constructed by combining an a.c. impedance spectrum, which is obtained normally over the higher frequency range (e.g., 5 to 13 MHz) by using a commercial impedance analyzer (e.g., HP 4192A), with the other which is obtained normally in the lower frequency range (<1 Hz) by Fourier-Laplace transforming the d.c. relaxation results. The partial ionic conductivity can then be extracted from the Warburg impedance at the lowest frequency region. The basic principle as well as experimental detail of the technique are given elsewhere.[5]

Nonstoichiometry (δ) was measured against oxygen partial pressure ($10^{-16} \leq Po_2/atm \leq 0.21$) and temperature

($900 \leq T/°C \leq 1100$) by thermogravimetry using a microbalance (Cahn D-200). A specimen of 0.45~0.5 g was suspended in a furnace with the aid of a Pt wire (0.2 mm thick) which was hung down from the microbalance. The temperature of the specimen was controlled within ± 1°C. Oxygen partial pressure around the specimen was controlled with N_2/O_2 gas mixtures (for the higher Po_2 values) or 90% N_2+10% CO/CO_2 gas mixtures (for the lower Po_2 values) under the total pressure of 1 atm. Here N_2 gas was employed as the background gas. Preliminary dummy test using an inert Al_2O_3-block showed that the weight was reproducible within ± 5 μg irrespective of gas compositions. The precision of each weight reading was better than 1 μg. Once the weight of the sample achieved a saturated value in a given gas mixture which was flowing around the specimen, the gas flow was then stopped and the sample weight was recorded. Weight change was determined by subtracting the reference weight in the air atmosphere at the identical temperature.

III. Results and Discussions

1. Total and partial conductivities

The total electrical conductivity (σ) and the partial ionic conductivity (σ_{ion}) vary with oxygen partial pressure at different temperatures as shown in Fig 1. The ionic conductivity falls in the range of 10^{-1} to 10^{-2} S/cm depending on oxygen partial pressure. The total conductivity may thus be regarded as essentially electronic (or $\sigma \approx \sigma_{el}$). As Po_2 decreases from 1 atm at a fixed temperature, the electronic electrical conductivity first remain little changed and then decreases. The former indicates that the majority electronic carrier (electron holes) is of extrinsic origin, i.e., their concentration is fixed by the B-ions, Ca_Y'. No sooner the conductivity reaches its minimum value (σ_{min}) than the oxide decomposes.

When a conductivity minimum is located on an electronic total conductivity isotherm ($\sigma_{el}=\sigma_p+\sigma_n$), one can distinguish more precisely the oxygen exponent of the electronic partial conductivity which bears the critical information on the defect structure[3] : The total (electronic) conductivity may be expressed in terms of the minimum conductivity and the partial conductivity ratio (α) as

$$\sigma = \sigma_{min}\cosh(1/2\ln\alpha);\ \alpha \equiv \frac{\sigma_p}{\sigma_n} = \frac{p}{nb} \tag{2}$$

where σ_p, and p are, respectively, the partial conductivity and the concentration of holes, σ_n, and n are the corresponding quantities for electrons, and b ($=\mu_n/\mu_p$) the mobility ratio of electrons to holes. One can thus easily reconstruct a total electrical conductivity isotherm into a plot of log α vs. log Po_2 Since $\sigma_p \propto p \propto P_{O_2}^{1/m}$ and $\sigma_n \propto n \propto P_{O_2}^{-1/m}$ on the assumption of the both mobilities being independent of Po_2, the slope of log α vs. log Po_2 is given as

$$\left(\frac{\partial \log \alpha}{\partial \log Po_2}\right)_T = \frac{2}{m} \tag{3}$$

One can thus determine the reciprocal oxygen exponent "m" from the slope of log α vs. log Po_2 with a precision twice higher than the conventional treatment. The result is shown in Fig. 2, where one can clearly distinguish three Po_2 regions, e.g., m=∞, at the higher Po_2 region, m=

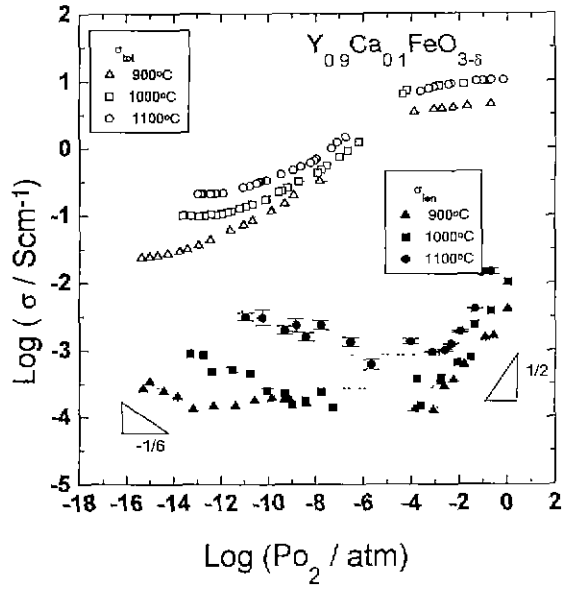

Fig. 1. The total conductivity (σ_{tot}) and ionic partial conductivity (σ_{ion}) of $Y_{0.9}Ca_{0.1}FeO_{3-\delta}$ vs. oxygen partial pressure (Po_2) at different temperatures.

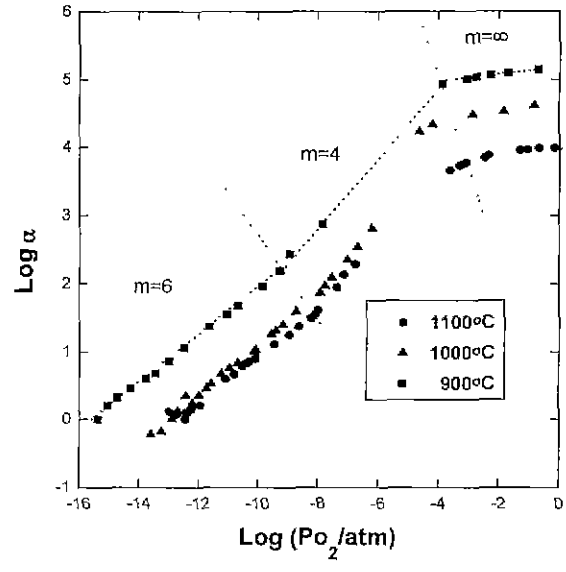

Fig. 2. Log α ($=\sigma_p/\sigma_n$) vs. log Po_2 at different temperatures. Note that the three regions of different values for the reciprocal oxygen exponents, m=6, 4, ∞, are clearly distinguished.

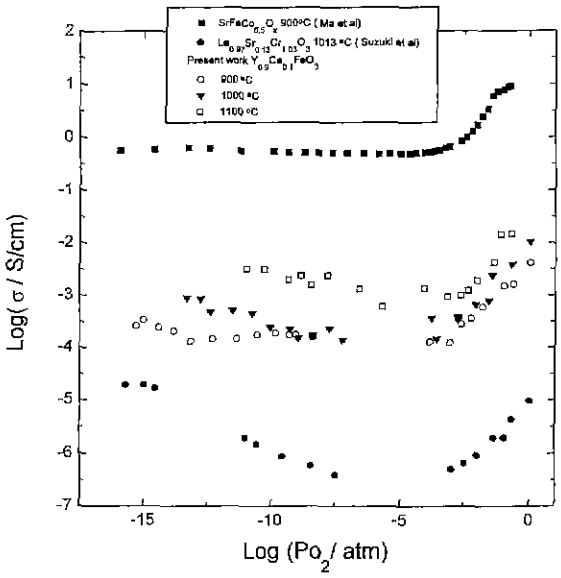

Fig. 3. Comparison of the ionic conductivity of $Y_{0.9}Ca_{0.1}FeO_{3-\delta}$ with those of similar oxides, $SrFeCo_{0.5}O_x$ (after Ma et al.[8]) and $La_{0.87}Sr_{0.13}FeO_{3-\delta}$ (after Suzuki et al.[9]). Note the inter-consistency in the variations with Po_2.

4 at the intermediate Po_2 region and m=6 at the lower Po_2 region.

It appears that the ionic conductivity also varies correspondingly in these three Po_2 ranges: $\partial\log\sigma_{ion}/\partial\log Po_2 \approx$ 1/2, 0 and -1/6, respectively, see Fig. 1. The ionic carrier of $Y_{0.9}Ca_{0.1}FeO_{3-\delta}$ has been identified as oxide anions via Tubandt-like electrotransport experiment that is detailed elsewhere.[7] It is thus suggested that the majority type of ionic defects be anti-Frenkel disorder, (O_i'', $V_O^{\cdot\cdot}$). An increase of the conductivity in the higher Po_2 region is then attributed to interstitial oxygen ions (O_i''). This picture has thus far been seldom considered for a perovskite structure.

Quite similar behavior of ionic conductivity with Po_2 has been reported for the other perovskite-based oxides, $SrFeCo_{0.5}O_x$,[8] and $La_{0.87}Sr_{0.13}Cr_{1.08}O_3$.[9] The results are compared with the present one in Fig. 3. It seems to be common to this type of oxides that, as Po_2 decreases, the ionic conductivity first decreases with a slope of 1/2, then remains flat, and finally increases with a slope of -1/6:The width of each Po_2 region, of course, depends on the composition of oxides. The increasing ionic conductivity with Po_2 in the higher Po_2 region has been interpreted as being due to oxygen interstitials in the former,[8] while in the latter as being due to grain boundaries.[9] The apparent correspondence of the variations of the electronic conductivity and the ionic conductivity in Fig. 1, however, indicates that the ionic conductivity variation as such is attributed to the bulk, not to the grain boundaries.

2. *Defect structure*

On the basis of the above information, one can easily envisage the defect structure of $Y_{0.9}Ca_{0.1}FeO_{3-\delta}$ and the like as

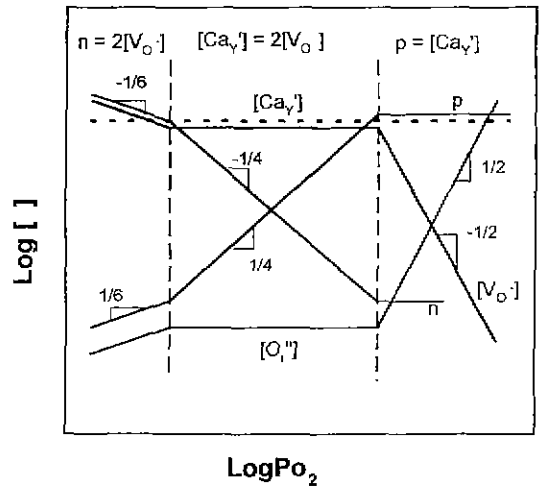

Fig. 4. Proposed defect structure of the system $Y_{1-x}Ca_xFeO_{3-\delta}$ based on anti-Frenkel disorder.

$$\text{nil} = e' + h^{\cdot} \qquad ; K_i = n\,p \tag{4}$$

$$O_O^X = O_i'' + V_O^{\cdot\cdot} \qquad ; K_F = [O_i''][V_O^{\cdot\cdot}] \tag{5}$$

$$1/2O_2(g) = O_i'' + 2h^{\cdot} \qquad ; K_{ox} = [O_i'']p^2 P_{O_2}^{-1/2} \tag{6}$$

in combination with the charge neutrality condition

$$n + 2[O_i''] + [Ca_Y'] = p + 2[V_O^{\cdot\cdot}] \tag{9}$$

where K_i (1=i, F, ox) denotes the equilibrium constant for the corresponding defect formation reaction and [k] the number of k-type structure elements per lattice molecule. In the above defect formation reactions, it is assumed that the point defects are ideally dilute.

The corresponding Brouwer diagram is shown schematlcaliy in Fig. 4. One can recognize that this defect structure explains reasonably well the measured total electrical conductivity and ionic conductivity provided that the oxygen interstitial has a higher mobility than the oxygen vacancy or $\mu_i > \mu_v$, and for the electronic carriers, $\mu_p > \mu_n$.

3. *Oxygen Nonstoichiomeiry*

At a given temperature, mass of the specimen oxide varies with Po_2 as shown in Fig. 5, where mass change relative to the (reference) mass in air, Δm is plotted. It is seen that, as Po_2 decreases from the air atmosphere, the mass little decreases down to log (Po_2/atm)$\approx$-3 and begins to decrease very rapidly from log (Po_2/atm)$\approx$-13, -10, -7 at 900°, 1000°, 1100°C, respectively, compared to the change in between. These demarcating Po_2-values appear to agree with those of the corresponding isotherms of ionic conductivity in Fig. 1. In accordance with the defect structure in Fig. 4, one may thus naturally assign the majority defect type ($V_O^{\cdot\cdot}$, Ca_Y') to the log (Po_2/atm)-regions, (-3,-13), (-3, -10) and (-3, -7) at 900°, 1000°, 1100°C, respectively. If it is the case, the electronic stoi-

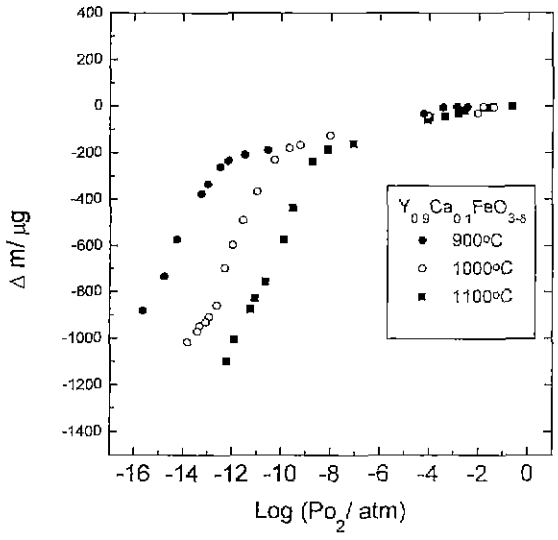

Fig. 5. Mass change relative to the the reference mass in air atmosphere, Δm vs. Po_2 at different temperatures.

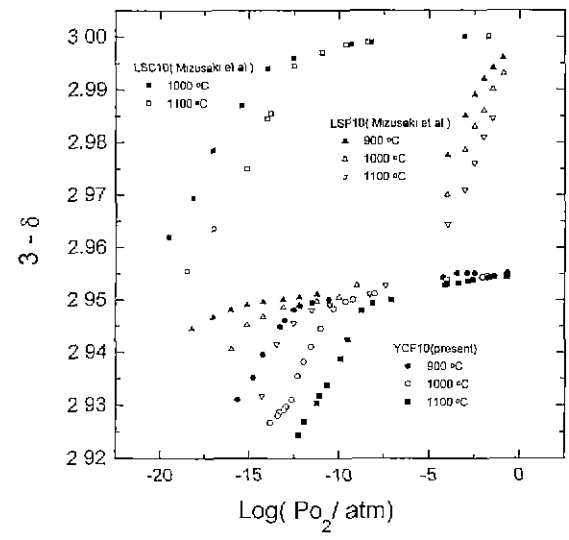

Fig. 6. Comparison of the oxygen content of $Y_{0.9}Ca_{0.1}FeO_{3-\delta}$ with those of other similar oxides, $La_{0.9}Sr_{0.1}CrO_{3-\delta}$ (LSC10, after Mizusaki *et al.*[11]) and $La_{0.9}Sr_{0.1}FeO_{3-\delta}$ (LSF10, after Mizusaki *et al.*[12]).

chiometric composition, where n≡p, will fall roughly at the center of each of these regions [say, log (Po_2/atm)≈-8, -6.5, -5 at 900°, 1000°, 1100°C, respectively]. The Δm-isotherms are, thus, expected to exhibit an inflection there[10] and the corresponding oxygen content to be 3-δ=2.95.

Upon increasing Po_2, log (Po_2/atm)≈-3 demarcates the two majority defect regimes, ($V_O^{\cdot\cdot}$, Ca_Y') and (Ca_Y', $h^{\cdot}$). It is, therefore, further expected that a nonstoichiometry (or Δm) isotherm should show an upturn towards another inflection at the ionic stoichiometric composition where $[O_i'']\equiv[V_O^{\cdot\cdot}]$ and 3-δ≡3.00. The rate of upturn is determined obviously by the ratio $r\equiv[O_i'']/[V_O^{\cdot\cdot}]$ at the boundary of the two defect regimes in Fig. 4 or the magnitude of K_F in Eq. (7): The ionic stoichiometric composition, 3-δ=3.00, will fall, e.g., at log (Po_2/atm)≈0, 1, 2 when $r=10^{-3}$ ($K_F\approx10^{-5}$), 10^{-4}($K_F\approx10^{-6}$), 10^{-5}($K_F\approx10^{-7}$), respectively. The present result, δm≈0 over the region ~-3≤ log (Po_2/atm)≤-0.67, implies that r or K_F must be very small or $r<<10^{-3}$ ($K_F<<10^{-5}$) intuitively This implication, in association with the ionic conductivity variation in the region of log $Po_2\geq$~-3 in Fig. 1, subsequently leads to another implication about the mobility ratio of oxygen interstitial to vacancy, that is, $\mu_i>\mu_v=1/r>>10^3$, which has never been reported earlier and looks even exotic for the crystallographic structure of the oxide in question. In order to elucidate this issue, determination of the absolute amount of oxygen content corresponding to the electronic stoichiometric composition is now under way.

Taking the value 3-δ=2.95 as the oxygen content in the middle of the defect regime of $[V_O^{\cdot\cdot}]=[Ca_Y']$, the present result is compared with the nonstoichiometry isotherms reported on the similar oxides, $La_{0.9}Sr_{0.1}CrO_{3-\delta}$ (dubbed as LSC10)[11] and $La_{0.9}Sr_{0.1}FeO_{3-\delta}$ (dubbed as LSF10)[12], as shown in Fig. 6. As is seen, the latter clearly exhibits an inflection at the electronic stoichiometric composition (at log Po_2/atm≈-13, -11, -9 at 900°, 1000°, 1100°C, respectively) and tends to another inflection at 3-δ=3.00, the ionic stoichiometric composition, at a Po_2 value apparently above 1 atm. It appears that the present data are rather consistent with the latter in the trend of variation with Po_2: Only the electronic stoichiometric composition is shifted towards the higher Po_2 values compared to LSF10 This inter-consistency tempts one to suspect that the oxygen content of LSC10 might have been overestimated: its quasi-flat region would rather correspond to 3-δ=2.95. Clearly more work is required to clarify this issue.

IV. Conclusion

For the system of $Y_{1-x}Ca_xFeO_{3-\delta}$, isothermal variations with Po_2 of electronic conductivity, ionic conductivity and nonstoichiometry are well explained in terms of the defect structure based on anti-Frenkel disorder. This defect picture, however, results in an unprecedented result of the electrochemical mobility of oxygen interstitials being much larger than that of oxygen vacancies ($\mu_i>\mu_v>>1000$), which is yet to be clarified.

References

1. N. Q. Minh, "Ceramic Fuel Cells", *J. Am. Ceram. Soc.*, **6**(3), 563-588 (1993).
2. J. Mizusaki, "Nonstoichiometry, Diffusion and Electrical Properties of Perovskite-type Oxide Electrode Materials", *Solid State Ionics* **52**, 79-91 (1992).
3. H.-I. Yoo and C.-S. Kim, "Electrical Properties and Defect Structure of $Y_{1-x}Ca_xFeO_3$ Orthoferrites", *Solid State Ionics*, **53/56**, 583-591(1992).
4. B Fu, W. Huebner, M. F. Trubelja and V. S. Stubican,

"$Y_{1-x}Ca_xFeO_3$: A Potential Cathode Material for Solid Oxide fuel Cell"; pp. 276-287 in Proceedings of the 3rd International Symposium on Solid Oxide Fuel Cell, Edited by S. C. Singhal, H. Iwahara. The Electrochemical Society, Pennington, NJ, 1993.

5. J.-S. Lee and H.-I. Yoo, "Direct Measurement of Partial ionic Conductivity of $Co_{1-\delta}O$ Via Impedance Spectroscopy Combined with dc Relaxation", *Solid State Ionics*, **68**, 139-149 (1994).
6. H. Becker and H. P. R. Frederikse, "Electrical Properties of Nonstoichiometric Semiconductor", *J. Appl. Phys. Suppl.*, **33**(1), 447-453 (1962).
7. C.-S. Kim and H.-I. Yoo, "A New Candidate for the Solid Oxide Fuel Cell Cathode, $Y_{0.9}Ca_{0.1}FeO_3$", *J. Electrochem. Soc.* **143**(9), 2863-2870 (1996).
8. B. Ma, U. Balachandran, J.-H. Park and C. U. Segre, "Electrical Transport Properties and Defect Structure of $SrFeCo_{0.5}O_x$", *J. Electrochem. Soc.* **143**(5), 1736-1744 (1996).
9. M. Suzuki, H. Sasaki and A. Kajimura, "Oxide Ionic Conductivity of Doped Lanthanum Chromite thin film interconnectors", *Solid State Ionics*, **96**, 83-88 (1997).
10. C. Wagner, "The Determination of Small Deviations from the Ideal Stoichiometric Composition of Ionic Crystals and other Binary Compounds", *Prog, Solid State Chem.*, **6**, 1-15 (1971).
11. J. Mizusaki, S. Yamaguchi, K. Fueki and A. Ishikawa, "Nonstoichiometry of the Perovskite-type Oxide $La_{1-x}Sr_xCrO_{3-\delta}$", *Solid State Ionics*, **12**, 119-124 (1984).
12. J. Mizusaki, M. Yoshihiro, S. Yamaguchi, K. Fueki, "Nonstoichiometry and Defect Structure of the Perovskite-type Oxide $La_{1-x}Sr_xCrO_{3-\delta}$", *J. Solid State Chem.*, **58**, 257-266 (1985).